Leakage Current Properties of PZT Thin Film Capacitors

Yoichiro MASUDA*, Takashi NOZAKA*, Hiroshi MASUMOTO**
and Takashi GOTO**

Abstract

Pb (Zr, Ti)O_3, Lead Zirconium Titanium oxide thin films were fabricated on Pt(111)/TiO_x/SiO_2/Si (100) and some oxide electrodes (SRO, IrO_2) on PZT thin films by the chemical solution deposition method, RF sputtering and PLD method. A leakage current and ferroelectric polarization switching in these PZT film capacitors were measured. We have discussed the nature of electrical conduction, and a fatigue of ferroelectric polarization switching in the PZT films. Therefore, it is clear that a variety of mechanisms, including surface-limited process such as Schottky, Poole-Frenkel, Space-Charge-Limited-Currents (SCLS) and the fatigue of polarization switching, are caused by a ferroelectric domain pinning effect.

Key words: Ferroelectric thin film, chemical solution deposition, leakage current density, fatigue, upper electrodes of platinum (Pt), $SrRuO_3$ (SRO) and IrO_2

1. Introduction

Ferroelectric thin films have recently attracted great interest as new dielectric materials for G-bit-scale ferroelectric random access memories (FeRAMs),[1] micro-electro-mechanical systems (MEMS),[2-4] pyroelectric detector, high frequency devices (RF-filter) and nonlinear optical thin films.

Many attempts on synthesis of ferroelectric thin films have been demonstrated by using chemical solution deposition method (CSD),[5,6] MOCVD,[7,8] RF magnetron sputtering,[9] a laser ablation technique[10,11] and Sol-Gel method so far.

Degradation of ferroelectric thin films, such as ferroelectric fatigue (the reduction of reversible polarization with repeated voltage cycles),[12,13] ferroelectric aging and resistance degradation, has been investigated and their mechanisms have been proposed. Since pinning and imprint effects associated with trapped electronic-charge and oxygen-Pb vacancies restrict the lifetime and reliability of the devices that utilize ferroelectric thin films, eliminating of these effects is important to realize FeRAMs and MEMS. Besides, degradation of ferroelectric is observed when a ferroelectric thin film is directly grown on a Si wafer, because various silicide compounds are synthesized. In order to overcome these problems, ferroelectric thin films have been grown on the oxide electrodes, such as RuO_2,[14] IrO_2,[15] $SrRuO_3$ (SRO), cubic perovskite La-Sr-Co-O (LSCO),[16] La-Ca-Mn-O (LCMO), La-Sr-Mn-O (LSMO),[17] as buffer layers.

In this study, Pb(Zr, Ti)O_3 (PZT) thin films are fabricated on Pt/TiO_x/SiO_2/Si substrates by using a chemical solution deposition method, and the capacitors with Pt, SRO and IrO_2 as top electrodes on the PZT thin films are made, then the polarization switching degradation, leakage current, the crystal structural and surface morphology of PZT thin films on different top electrodes are investigated.

2. Experimental Procedure

PZT films were deposited by the conventional sol-gel method. The solution used in this study was prepared by Mitsubishi Materials Corporation. The compositions of 15wt%PZT precursor were 52/48 in the Ti/Zr ratio. Pb content, Pb/Zr/Ti, was 115/52/48.

Pt(200 nm)/TiOx(40 nm) bottom electrodes were deposited on the SiO_2/Si(100) wafers used in this experiment and the wafers were supplied by Seiko-Epson Co.. PbTiO_3 (1wt% PT=115/100) was used to crystallize PZT thin films. PT precursors were spin-coated on the Pt(111)/TiOx/SiO_2/Si(100) substrate at 500 rpm for 5 s and continuously at 3,000 rpm for 30 s.

Then the films were pyrolyzed at 300°C for 3 min in air on a temperature-fixed hot plate, and placed on a cooling plate. The thickness of the PT seeding layer after annealing was 80 nm.

平成15年12月26日受理

* Department of Electrical and Electronics Engineering, Graduate school, Hachinohe Institute of Technology 88-1, Ohbiraki, Myo, Hachinohe, Aomori 031-8501, Japan

** Institute for Material Research, Tohoku University 2-1-1 Katahira, Aoba-ku, Sendai, Miyagi, 980-8577, Japan

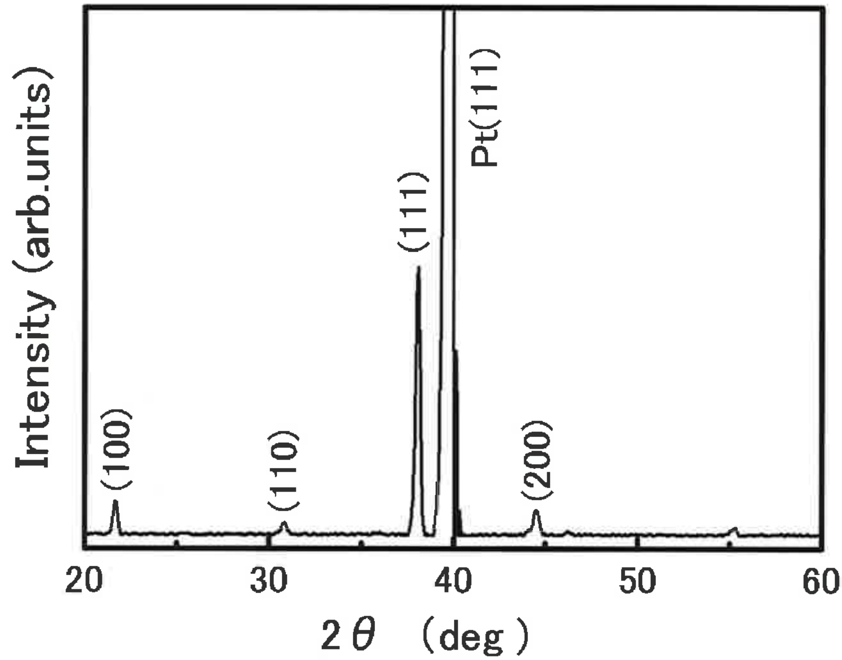

Figure 1. X-ray diffraction patterns of PZT thin films deposited on Pt/TiOx/SiO_2/Si(100).

PZT solutions were spin-coated on the substrates at 500 rpm for 5 s and continuously at 3,000 rpm for 30 s. Then the films were dried at 100°C for 5 min, pyrolyzed at 300°C for 3 min in air on a temperature-fixed hot plate, and placed on a cooling plate. Then the films were annealed in O_2 at 700°C for 2 min by rapid thermal annealing (RTA) to fabricate PZT single-coated films. PZT multicoated films were prepared by repetitions of this PZT deposition process up to the desired film thickness. The crystal structure of the thin films was examined by an X-ray diffract meter (Rigaku RAD-3C). The electrodes of 0.3 mm ϕ on the specimens used for electrical measurements were post-annealed at 700°C for 2 min.

The i-V characteristics were determined by using a pA meter (Advantest-TR8652). After a 0.1 V step voltage was applied to the thin film samples for 1 s, the leakage currents of the thin films were measured. The P-E hysteresis curves and fatigue properties were examined by using a ferroelectric test system (Radiant Technologies) at 8 V and 500 kHz pulse wave.

3. Results and Discussion

Figure 1 shows the X-ray diffraction (XRD) pattern of the PZT thin films deposited on PT/Pt/TiOx/SiO_2/Si(100). As shown in the figure, XRD pattern of PZT thin film on the Pt substrate shows that the material is of tetragonal phase, and that there is preferential ordering along ⟨111⟩ direction.

Figure 2 shows the AFM image of PZT thin film on Pt/TiOx/SiO_2/Si(100) substrate. The average surface roughness is Ra=6.46 nm. This film shows good microstructure with no pinholes and micro cracks.

Figure 3 shows ε_S-V property of Pt/PZT/Pt/TiOx/SiO_2/Si, IrO_2/PZT/Pt/TiOx/SiO_2/Si and SRO/PZT/Pt/TiOx/SiO_2/Si capacitors at 1 kHz. Relative dielectric constants ε_S of every specimen

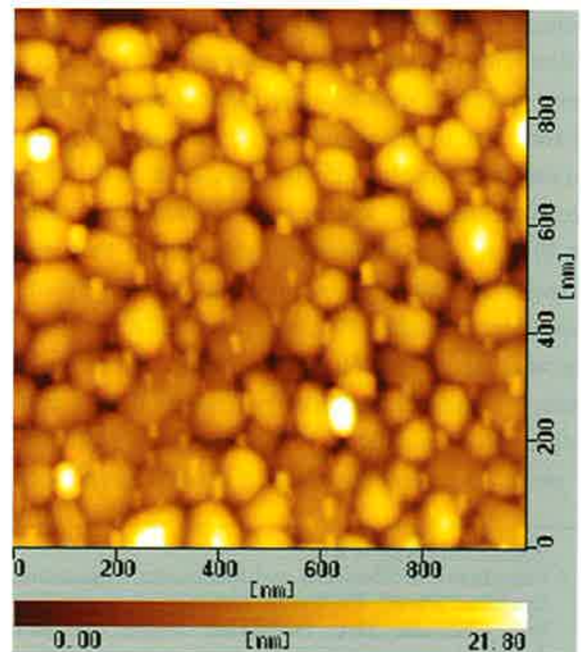

Figure 2. AFM image of PZT thin films on Pt/TiOx/SiO_2/Si(100) substrate.

showed the peak value of symmetrical property. This peak appears in the field corresponding to the coercive field. This is considered to be caused by the 180°domain switching. As X diffraction analysis shows, 90° domain does not exist in these thin film materials.

Figure 4(a), (b) and (c) show the logarithmic plot of the i-E relation-ship for (a) Pt/PZT/Pt/TiOx/SiO_2/Si, (b) IrO_2/PZT/Pt/TiOx/SiO_2/Si and (c) SRO/PZT/Pt/TiOx/SiO_2/Si capacitors. The value of i increases abruptly from 10^{-8} to 10^{-3} A・cm^{-2} with increasing of E up to 200 kV・cm^{-1}. The thin semi-conductive ferroelectric layer appears on the surfaces of IrO_2/PZT and Pt/PZT, and the leakage current shows the rectifier characteristics. The cause of the appearance of the negative resistance property seems to be the charge injection in this field. Besides, on the surface of SRO/PZT, the large leakage current flows

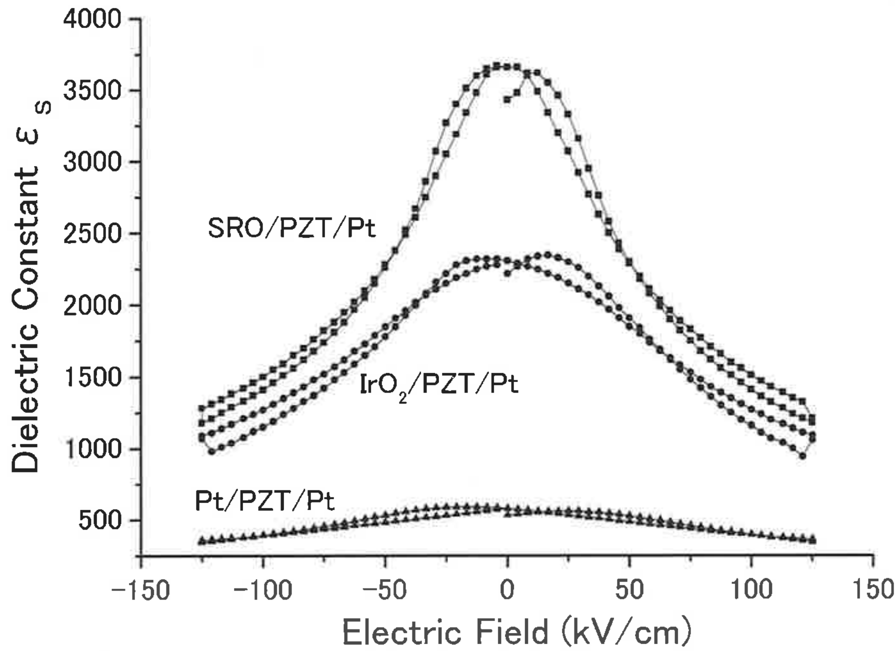

Figure 3. ε_s-V property of Pt/PZT/Pt/TiOx/SiO_2/Si, IrO_2/PZT/Pt/TiOx/SiO_2/Si and SRO/PZT/Pt/TiOx/SiO_2/Si capacitors at 1 kHz.

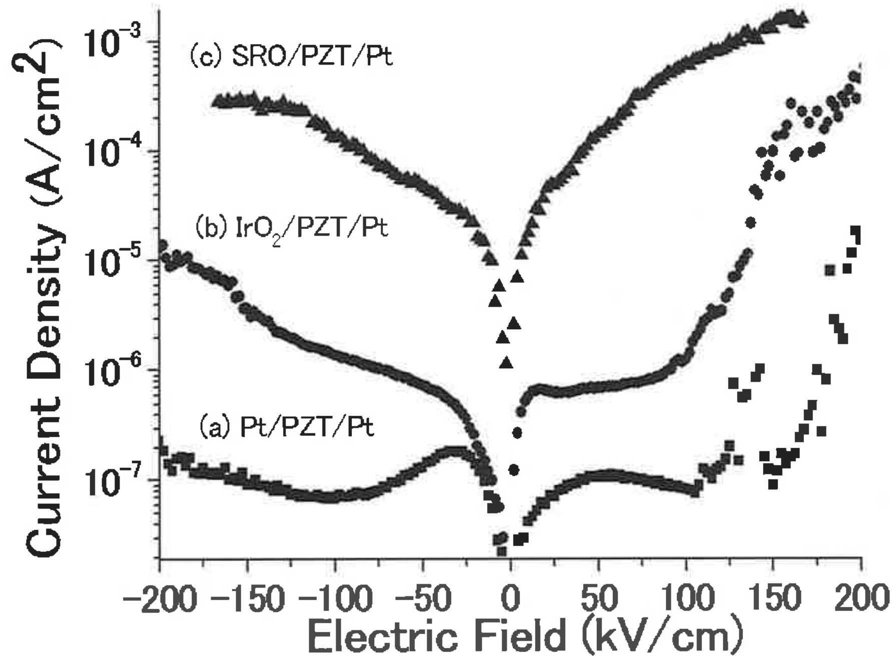

Figure 4. Logarithmic plots of the I-E relationship for (a) Pt/PZT/Pt/TiOx/SiO_2/Si, (b) IrO_2/PZT/Pt/TiOx/SiO_2/Si, and (c) SRO/PZT/Pt/TiOx/SiO_2/Si capacitors.

by Space-Charge-Limited Currents (SCLC) and Fowler-Nordheim Current.

These results can be explained in terms of the generated space charge current between the ferroelectric films and electrodes. The leakage current density of the $Pt/PZT/Pt/TiOx/SiO_2/Si$, $IrO_2/PZT/Pt/TiOx/SiO_2/Si$ and $SRO/PZT/Pt/TiOx/SiO_b/Si$ thin film capacitors is estimated to be 350 $\mu A \cdot cm^{-2}$, 500 $\mu A \cdot cm^{-2}$ and 30 $mA \cdot cm^{-2}$ at 50 $kV \cdot cm^{-1}$ applied field, respectively. It is found that the leakage currents of the thin film capacitors using the IrO_2 and SRO electrodes show 10～100 times larger than that of the capacitor using the Pt electrode. Schottky barrier appears on the surfaces of PZT thin films and top electrodes. As a result, Schottoky currents and Fowler-Nordheim Currents flow as the surface limited currents. This can be considered to be the cause of the asymmetry of the leakage currents[1]. However, it is difficult to explain the cause of increase of the leakage currents in the oxide electrodes (SRO, IrO_2) because the detailed analyses of the chemical bonding of PZT thin films and the oxide electrodes have not been made by XPS and SIMS.

Figures 5(a) and (b) show the band-structure of PZT and Pt before and after Pt electrode and n-type PZT semi-conductor are connected, and the Schottky barrier height is calculated using the parameters of each value from the references. When Pt electrode and n-type PZT thin film are connected, the band structure bends like Fig. 5(b), as the Fermi level of metal and that of semiconductor are in good agreement, and the Schttoky barrier is made on the surface of the Pt/PZT thin film.

The Ideal Schottky barrier height Φ_B is shown as formula (1), where Φ_M is the work function of metal and χ_S is electron affinity of PZT.[18]

$$\Phi_B = \Phi_M - \chi_S \qquad (1)$$

The Schttoky barrier of Pt/PZT thin film surface is 1.8 eV from formula (1). The work function of IrO_2 and SRO is about 4.6 eV, therefore, by using IrO_2 and SRO electrodes, the Schottky barrier height is lowered 0.7 eV in comparison to Pt/PZT thin film, and leakage currents of IrO_2/PZT and SRO/PZT thin films increase.

Figure 6 shows the leakage current property in the form of Schottky-plot when the upper electrodes of PZT/PT/Pt(111)/$TiOx/SiO_2$/Si(100) thin films are changed. When Pt and IrO_2 are used for the upper electrodes, the Ohmic property is shown in the lower electric fields, and the leakage currents are saturated to about 100 kV/cm, and then the linearity similar to the Schottky current appears. In the case of the leakage current of SRO thin film electrode on PZT thin film, Space-Charge-Limited Currents (SCLC) and Fowler-Nordheim Current are observed. When IrO_2 and SRO electrodes are used, it seems that Schottky barrier height is lowered and the leakage currents increase responding to the work function of metal. However, the leakage current of SRO thin film electrode on PZT thin film increases on a few orders. The cause of the difference seems to be the

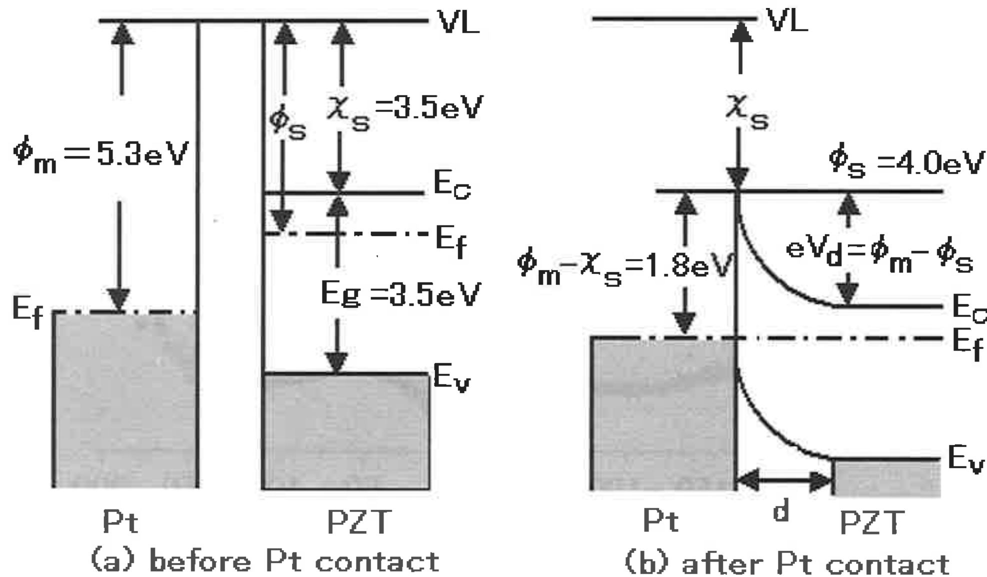

Figure 5. Band structure in PZT/Pt capacitor (a) before and (b) after contact.

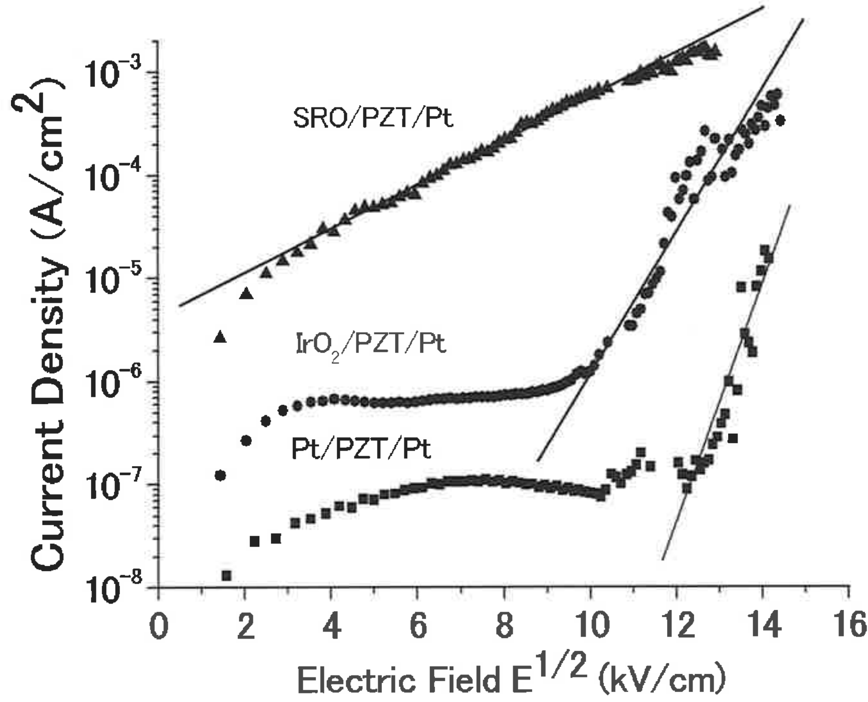

Figure 6. Leakage current property in the form of the Schottky plot for PZT thin films.

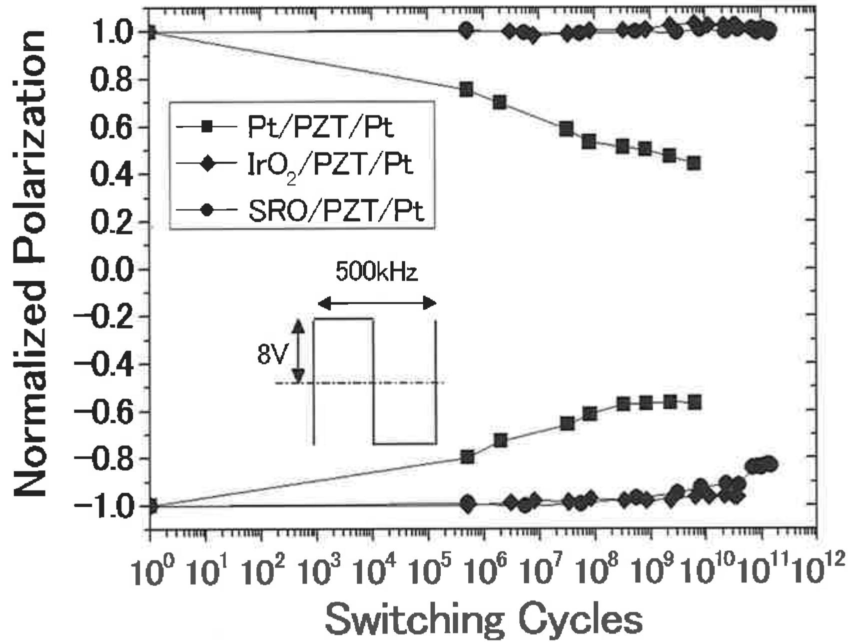

Figure 7. Polarization fatigue performance of $Pt/PZT/Pt/TiOx/SiO_2/Si$, $IrO_2/PZT/Pt/TiOx/SiO_2/Si$, and $SRO/PZT/Pt/TiOx/SiO_2/Si$ thin-film capacitors at the bipolar voltage switching cycles of ± 8 V (500 kHz).

difference of the method: the RF magnetron sputtering method is used for Pt and IrO_2 electrodes and pulsed laser deposition method is used for SRO electrode, that is, the barrier condition of the surfaces of electrode and PZT thin film can be the cause of the difference.

The Schottky currents are generally shown in formula (2) and the currents depend on the work function of metal and temperature. The characteristic of temperature of these currents, or the measurement of XPS and SIMS, must be investigated to know the mechanisms of them.

$$J = AT^2 \exp\{-q\Phi_B/kT\} \quad (2)$$

Where, A, q, k and T are Richardson-Dushman conatant, electric charge, Boltzemàn constant and

absolute temperature, respectively.

Figure 7 shows the polarization fatigue performance of $Pt/PZT/Pt/TiOx/SiO_2/Si$, $IrO_2/PZT/Pt/TiOx/SiO_2/Si$ and $SRO/PZT/Pt/TiOx/SiO_2/Si$ thin film capacitors, at switching cycles of ±8V (500 kHz). As shown in the figure, the remnant polarization value of the PZT thin film of $Pt/PZT/Pt/TiOx/SiO_2/Si$ thin film capacitor decreases to 50% of initial value at 10^8 switching cycles, while Pr value of PZT thin films of $SRO/PZT/Pt/TiOx/SiO_2/Si$ and $IrO_2/PZT/Pt/TiOx/SiO_2/Si$ thin film capacitors remained constant at more than 10^{11} switching cycles. Degradation of the PZT thin film is not observed while using the SRO and IrO_2 thin film electrodes as buffer layers.[19]

The loss of switching polarization with repeated polarization reversal is due to pinning of the domain wall, which inhibits switching of the domain affected by induced internal space charge at domain boundaries. However, a variety of mechanisms for domain wall pinning have been proposed, including pinning due to electron charges trapped by oxygen vacancies.[20]

From these results, it is confirmed that the polarization ferroelectric fatigue property of the PZT thin film is improved by using the SRO and IrO_2 thin film electrodes as buffer layers.

4. Conclusions

By CSD method, we fabricated the PZT capacitors whose upper electrodes were changed into Pt, IrO_2 and SRO.

It is found that the leakage currents of the thin film capacitors using the IrO_2 and SRO electrodes are 10 ～100 times larger than that of the capacitor using the Pt electrode.

The cause of this can be considered to be the formation of semi-conductive PZT thin film and complex compound layer on the surfaces of the thin film oxide electrode and PZT thin film. In future, the characteristics of this phenomenon will be explained by XPS and SIMS analyses.

The remnant polarization values of $Pt/PZT/PT/Pt(111)/TIO_X/SiO_2/Si(100)$ capacitors decrease to 50% of initial value by domain polarization switching of 10^8 cycles. This was caused because space charge appeared, internal electric field was formed and spontaneous polarization was pinned in the PZT thin film by oxygen defect and PbO vacancies. The degradation of the polarization values was not observed on 10^{11} cycles when SRO and IrO_2 electrodes were used as top electrodes.

As a result of this study, we found that oxide electrodes can be effective materials for FeRAM and MEMS devises.

Acknowledgements

This work was supported by Laboratory for Developmental Research of Advanced Materials, Institute for Material Research, Tohoku University and the authors would like to thank Prof. Tetsunori Takahashi for his useful discussions.

Reference

1) J.F. Scott : Ferroelectric Memories ; Springer Series in Advanced Microelectronics-3 March (2000)
2) N. Setter : Piezoelectric Device April (2000)
3) H. Maiwa and N. Ichinose : Jpn. J. Appl. Phys. 39 (2000) 5403
4) K. Kakimoto, H. Kakimoto, S. Fujita and Y. Masuda : J. Amer. Ceram. Soc. 85, 4 (2002) 1019
5) K. Maki, N. Soyama, S. Mori and K. Ogi : Jpn. J. Appl. Phys. 39 (2000) 5421
6) T. Iijima, G.H.Z. Wang, H. Tsuboi, K. Hiyama and M. Okada : Jpn. J. Appl. Phys. 39 (2000) 5426
7) Y. Takashima, K. Tanaka and Y. Sakabe : Jpn. J. Appl. Phys. 39 (2000) 5389
8) H. Fujisawa, K. Morimoto, M. Shimizu and H. Niu : Jpn. J. Appl. Phys. 39 (2000) 5446
9) Y. Fukuda and K. Aoki : Jpn. J. Appl. Phys. 36 (1997) 5739
10) H. Kakemoto, K. Kakimoto, A. Baba, S. Fujita and Y. Masuda : J. Ceram. Soc. Jpn. 109. 8 (2001) 651
11) Z.J. Wong, K. Kikuchi and R. Maeda : Jpn. J. Appl. Phys. 39 (2000) 5413
12) T. Nishida, S. Okamura, T. Shiosaki, S. Fujita and Y. Masuda : Jpn. J. Appl. Phys. 38 (1999) 5337
13) Y. Masuda, S. Fujita, T. Nishida, H. Masumoto and T. Hirai : Proc. 11th IEEE, Swtzerland (1998) 23
14) S.K. Hong, H.G. Yang and H.J. Kim : J. Korean Phys. Soc. 32 (1998) 1525
15) C.H. Kim and M. Lee : Korean Ceram. Soc. Bull. 23. 5 (2002) 741
16) F. Mcnall, J.H. Kim and F.F. Lange : J. Mater. Res. 15. 7 (2000) 1546
17) K.V. IM, B.J. Kuh, S.O. Park, S.I. Lee and W.K. Choo : Jpn. J. Appl. Phys. 39 (2000) 5437
18) J.F. Scott : Jpn. J. Appl. Phys. 38(19999) 2272
19) W.L. Warren, D. Dimons and R.M. Warser : Mat. Res. Soc. Bull. 21.7 (1996) 40
20) W.L. Warren, D. Dimons, B.A. Tuttle, G.E. Pike, R.W. Schwartz, P.J. Clews and D.C. MacIntry : J. Appl. Phys 77 (1995) 1400